Self-focusing in High-Power Optical Fibers

G. Ronald Hadley and Arlee V. Smith
P. O. Box 5800, Sandia National Laboratories, Albuquerque, NM 87185

Abstract

Recently the use of "vortex" beams of high azimuthal mode number has been proposed as a way of increasing the maximum peak power through-put of optical fibers beyond the few MW allowed for Gaussian beams by self-focusing. We report a numerical investigation of these and other schemes using a beam propagation approach that includes a Kerr-type nonlinearity.

I. Introduction

Self-focusing of laser beams in Kerr media has been studied in bulk samples for over three decades, and during the mid-70's was recognized to be the primary mechanism limiting the maximum power that could be extracted from the glass amplifier rods common in laser fusion experiments[1]. This critical power is given for Gaussian beams by the formula[2]

$$P_{cr} = \frac{3.77\lambda^2}{8\pi n_0 n_2} \tag{1}$$

where λ is the vacuum wavelength, and the index of refraction of the medium in the presence of an optical field of intensity I is expressed as

$$n = n_0 + n_2 I \ . \tag{2}$$

Optical beams whose powers are greater than P_{cr} have been shown both theoretically and experimentally to collapse, regardless of their initial diameter, until damage occurs.

One of the more fruitful and interesting attempts at exceeding this limit involves the propagation of beams with angular momentum, the so-called "vortex" beams[3]. Self-similar solutions of the nonlinear Schrodinger Equation have been constructed for such beams in which the optical intensity is concentrated into a ring around the beam center whose width decreases as the "vorticity" of the beam increases. These solutions show propagation in bulk media at many times the critical power at least for some distance, but were determined both theoretically and experimentally to be unstable, and eventually collapse into multiple filaments at the radius of the ring[3]. Thus for propagation in bulk media the critical power has proven to be a difficult limit to exceed.

More recently, this question as arisen anew, albeit in a slightly different fashion, as workers have begun to examine the maximum power transmittable through an optical fiber[4]. Knowledge of power limitations to light propagation through optical fibers is important in the development of fiber amplifiers and for the delivery of laser light to precise positions for materials processing. In this case the light is no longer freely diffracting, but rather is guided in a circular dielectric waveguide. In this work, we investigate theoretically the propagation of laser beams of various modal shapes and

Integrated Optics: Devices, Materials, and Technologies XI, edited by Yakov Sidorin, Christoph A. Waechter,
Proc. of SPIE Vol. 6475, 64750G, (2007) · 0277-786X/07/$18 · doi: 10.1117/12.706132

super-critical powers through step-index optical fibers, with the goal of raising the maximum stable power attainable. Our tool for this investigation is a numerical model employing the finite difference beam propagation method on a triangular grid. The latter technique is used to avoid stair-casing errors in resolving the circular fiber core. In successive sections we will give a brief description of the model equations and then describe the results and conclusions of this work.

II. Propagation Equation

Due to the small index contrast present between the fiber core and cladding, we keep only a single component of the optical field, say H. Then wide-angle beam propagation in the Pade(1,1) approximation is expressable as[5]

$$(1+\xi P)H^{n+1} = (1+\xi^* P)H^n \tag{3}$$

where $\xi = -\frac{i\Delta z}{4k} + \frac{1}{4k^2}$, Δz is the propagation step size, $k = \bar{n}k_0 = \frac{2\pi\bar{n}}{\lambda_0}$ is the reference wavevector, and

$$P \equiv \nabla_\perp^2 + k_0^2(\varepsilon - \bar{n}^2)\,. \tag{4}$$

In Eq. (3), the superscript on the field denotes the propagation plane with propagation in the z direction, and in (4) $\varepsilon(\mathbf{x}) = n^2$ is the dielectric constant of the fiber, with the index of refraction n as defined in Eq. (2) above. We difference Eq. (3) on a topologically regular triangular grid[6], and solve the resulting finite difference equations using standard sparse matrix routines. Runtimes for the problems discussed in this article are typically about 30 minutes on a Hewlitt-Packard xw9300 workstation.

III. Simulation Results

(a) Fundamental fiber mode

All simulations described below involved propagating an eigenmode of the 25-μm-diameter step-index circular fiber centered on a 44-μm square problem region as shown in Fig. 1. The 220 x 220 triangular grid was constructed using an automatic grid generator that positioned the closest grid points exactly on the circle representing the fiber core-cladding interface, while other grid points were allowed to move during generation so as to result in the most regular grid. This procedure resulted in a very accurate resolution of the circular region so as to minimize stair-casing errors. The wavelength of the light was 1.064 μm, the refractive indices of the core and cladding were 1.45313 and 1.44968, resp., and the nonlinear index n_2 was 2.7 x 10^{-16} cm^2/W, a value typical of glass fibers.

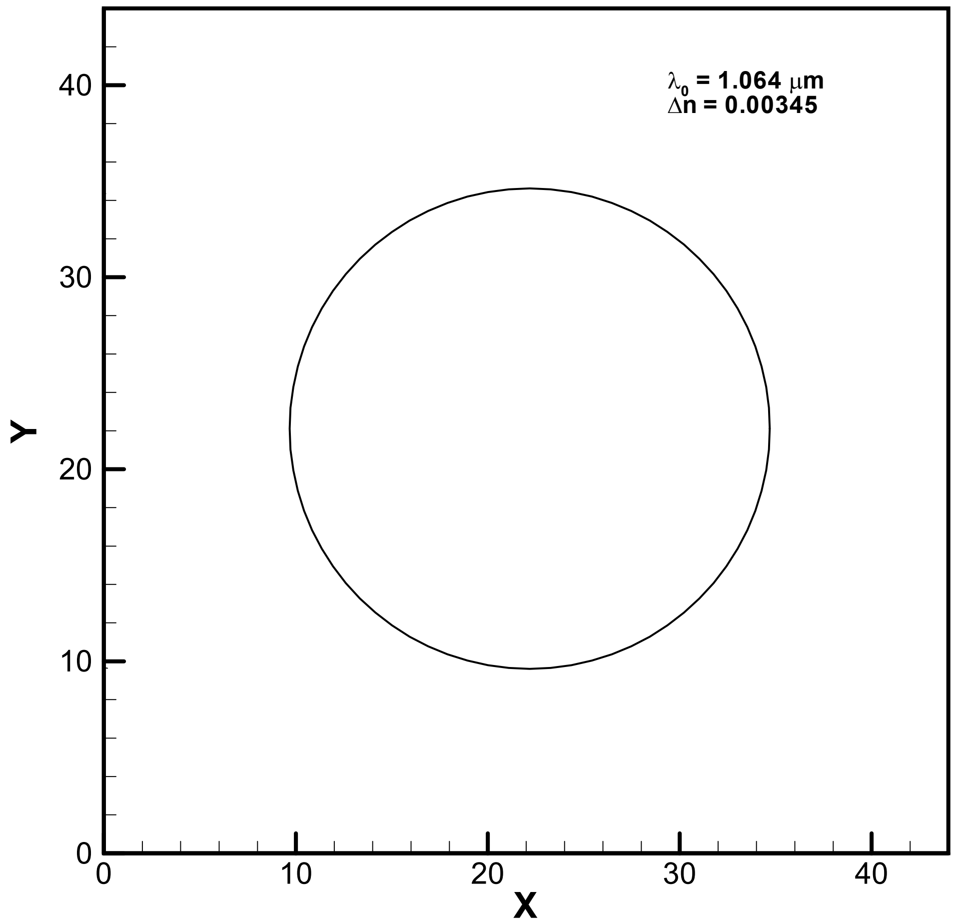

Fig. 1. Schematic of problem region employed for numerical calculations described in the text. All distances are in μm.

Our initial investigation was to check the formula (1) for the fundamental fiber eigenmode and see if the confinement by the fiber core-cladding interface caused any significant changes to the critical power. We computed the linear fiber eigenmode using a separate computer program with $n_2 = 0$ but employing exactly the same grid as for the propagation. The resulting eigenmode was then scaled to a power of 3 MW and propagated with a small fictitious gain to affect a gradual increase in power in order to avoid sudden changes in beam profile due to the presence of the nonlinearity. Upon reaching a predetermined power, the gain was removed and the beam was then propagated until it was determined whether a self-focusing event occurred. Of course, this brings up an immediate problem common to all the calculations reported here: How long a propagation length is sufficient to say for certainty that no self-focusing event will occur? With a propagation step size of 5 μm, 2000 steps per cm were required, resulting in significant runtimes. Consequently, propagation lengths were limited to about 2.5 cm, and the conclusions reported here are based on lengths of that size. It is certainly possible that some of the numbers might change and self-focusing might occur if propagation were continued to longer distances. However, when the waveform constricted to several small lobes that moved and changed size, maintaining good energy conservation was difficult much beyond the range employed here. Consequently, propagation to still longer distances was of dubious value.

The results for the fundamental eigenmode showed self-focusing at a power of 4.3 MW, very close to the value of 4.33 obtained from Eq. (1). Of course, exact agreement is not expected since Eq. (1) is valid only for a Gaussian profile. But we expected that the slight difference in profile between a Gaussian and the fiber mode would not make a noticeable difference in the critical power, and that proved to be the case. Also, this calculation confirmed the suspicion that confinement by the fiber made virtually no difference. This result is understandable by considering that once the mode starts to constrict under the action of self-focusing, the mode shrinks from the core-cladding interface and propagates as if it were in a bulk medium.

(b) Higher-order fiber modes with $L = 0$

An obvious common-sense approach to increasing the critical power appears to be the use of higher-order fiber modes, since (1) the power is divided among several lobes, each of which may be considered to support one critical power, and (2) the fiber index profile will keep the modes confined, in contrast to a bulk medium that would allow them to diffract rapidly and thus be of little use. These modes are of the form $f_m(r)\cos(m\theta)$ and $f_m(r)\sin(m\theta)$, where $f_m(r)$ is a Bessel function that is zero at the fiber origin and peaks just inside the core-cladding interface, matched to a modified Bessel function outside the interface. The width of the peak region decreases with increasing *m*. These modes have zero angular momentum, as will be discussed in detail below.

Following the above logic, we might expect the $m = 1$ mode to support about 8.6 MW of power before self-focusing. Propagation simulations for this mode did indeed confirm this logic in the sense that around 8.6 MW both lobes self-focused independently as expected. However, below this power, the two-lobed pattern eventually coalesced into a single lobe within a distance of 7-14 mm, and then that lobe self-focused as usual. Thus, the higher-order mode fared essentially no better than the fundamental, with an initial power of 4.5 MW coalescing into a single lobe and self-focusing at 1.62 cm.

This behavior can be better understood by examining the propagation of light down a double-moded nonlinear slab waveguide. Without the nonlinearity, a given eigenmode of the waveguide will of course propagate forever without change. However, the presence of the Kerr nonlinearity leads to very different behavior as shown in Fig. 2. If we initially inject the antisymmetric mode at some high power, the waveguide immediately changes its refractive index profile to contain two local maxima under the peaks shown in Fig. 2a. A slight imbalance in power between the two peaks causes an imbalance in refractive index, which in turn changes the mode set. An additional exchange of power further increases the index imbalance (Figs. 2b,2c) and the power transfer intensifies until finally one waveguide captures essentially all the power (Fig. 2d), at least for a short distance. If the power in that lobe is greater than the critical power, then self-focusing is likely to occur.

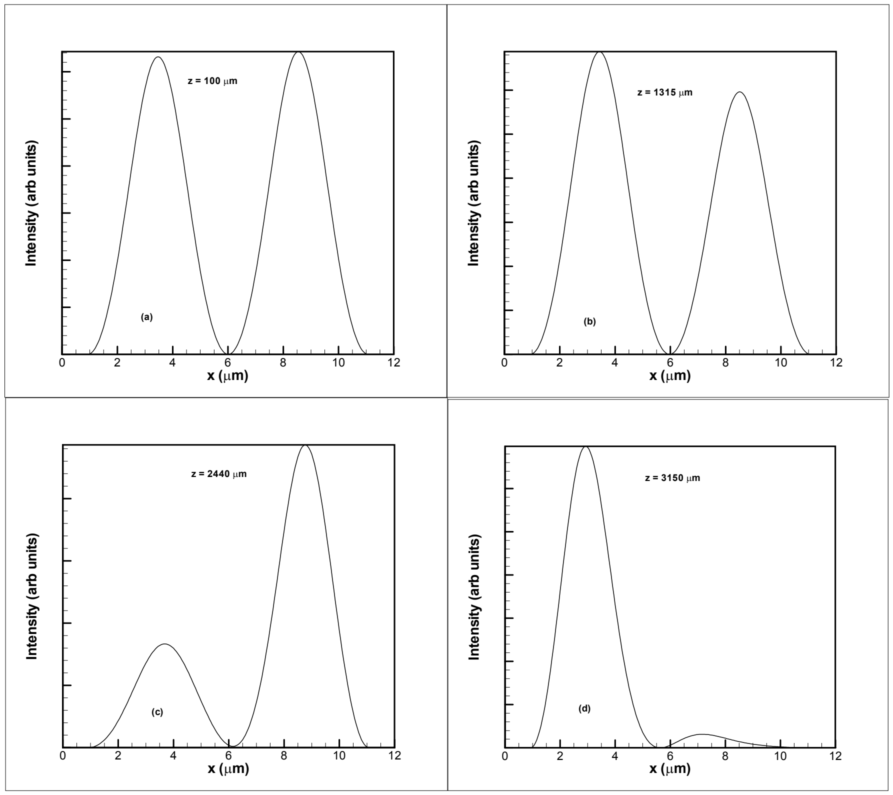

Fig. 2. Propagation of the antisymmetric eigenmode of a two-moded nonlinear waveguide. The waveguide is bounded by electric walls at 1 and 11 μm.

Returning to the fiber problem, additional calculations performed starting with the $m = 2$ and $m = 3$ modes showed similar behavior, with the initial multi-lobed pattern eventually coalescing into a single mode, and that mode then proceeding to a collapse. It is not clear whether the critical power for the higher-order modes is identical to that for the fundamental, or slightly higher since 5.5 MW cases were observed to propagate without self-focusing. What is clear is that the critical power is not substantially higher for these cases, certainly not scaling with the number of lobes in the mode pattern.

(c) Modes with $L \neq 0$

Recently, investigations into the propagation behavior of circular beams with angular momentum (so-called "vortex" modes) have shown somewhat stable propagation at powers well above the critical power[3]. In particular, the authors in reference 3 find a new critical power for modes with angular momentum that is

$$P_{cr}^{(m)} = \frac{2^{2m}\Gamma(m+1)\Gamma(m+2)}{\Gamma(2m+1)} P_{cr} . \qquad (5)$$

This formula indeed represents a significant enhancement, since, for example, $P_{cr}^{(5)} = 24.38 P_{cr}$. However, it is unclear from reference 3 to what degree the ring modes corresponding to higher values of m are stable against filamentation, even for powers well below $P_{cr}^{(m)}$. In any case, their results certainly excite curiosity and justify an investigation for fiber modes with angular momentum.

The angular momentum operator is given by[7] $\mathbf{L} = \frac{1}{i}(\mathbf{r} \times \nabla)$, and thus the component in the direction of propagation is $L_z = -i\frac{\partial}{\partial \theta}$ and the measured value of angular momentum is

$$\langle L_z \rangle = -i \frac{\int H^* \frac{\partial H}{\partial \theta} dA}{\int H^* H dA} \tag{6}$$

Thus for the modes described above, $H = f_m(r)\cos(m\theta)$ and

$$\langle L_z \rangle = -i \frac{\int f_m^* f_m dr \int_0^{2\pi} -m\cos(m\theta)\sin(m\theta) d\theta}{\int f_m^* f_m dr \int_0^{2\pi} \cos^2(m\theta) d\theta} = 0 . \tag{7}$$

On the other hand, the modes $f_m(r)e^{\pm im\theta}$ are eigenstates of L_z with eigenvalues $\pm m$. The latter quantity is also sometimes referred to as the *topological charge* of the mode[3], and should be conserved during propagation so long as the dielectric constant is independent of θ.

We have performed calculations similar to those described in the previous section with modes of nonzero m in order to assess the effects of angular momentum on the self-focusing behavior of the mode. To this end, we prepared the initial mode by computing the sum $f_m(r)\cos(m\theta) + if_m(r)\sin(m\theta)$ where the two real components are found from the eigenmode solver as usual and stored in a data file. Although the two modes are degenerate, the solver can be "nudged" towards one or the other by applying a small dielectric constant perturbation that breaks the degeneracy. The composite mode was found to propagate initially with only minor shape changes, followed by an unstable coalescence into one or two major lobes, as before. The topological charge as computed from Eq. (6) was found to be conserved to high accuracy during propagation until such time as the beam exhibited features with high spatial frequency, at which point the charge would typically decrease somewhat. However, now a new behavior surfaced in which the lobes were found to precess around the periphery of the fiber core, as illustrated in Fig. 3 for the case $m = 1$.

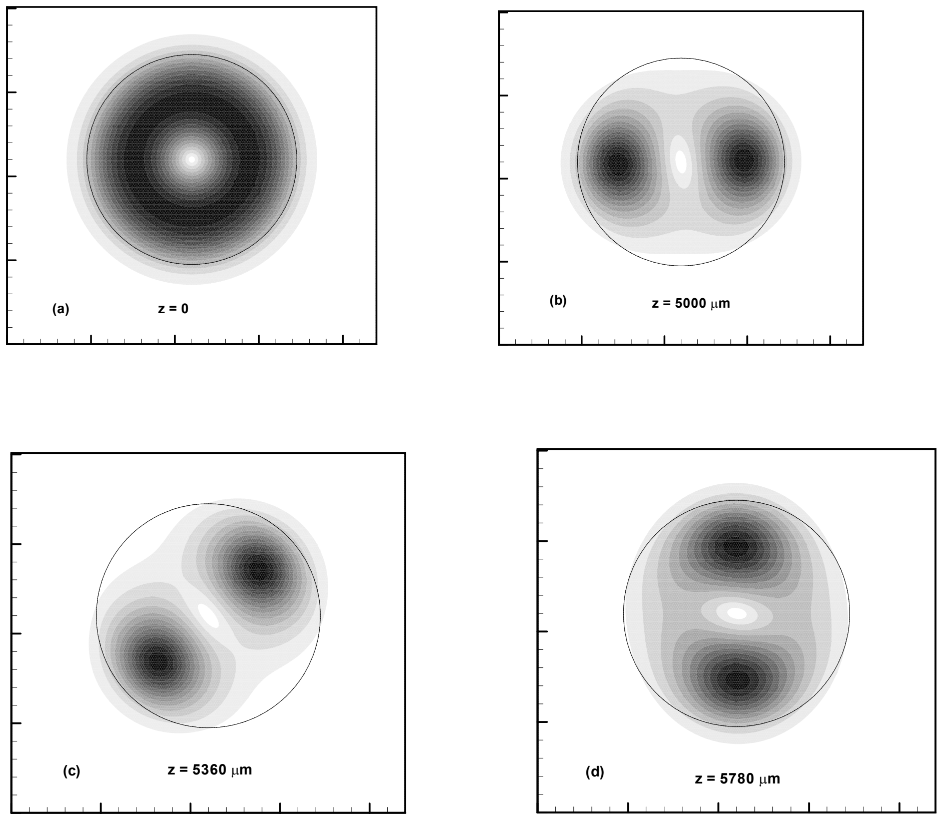

Fig. 3. Precession of the major lobes for the $m = 1$ fiber eigenmode, as seen in snapshopts of the beam intensity contours at several propagation distances. (a) initial profile, (b) z = 5 mm, (c) z = 5.36 mm, (d) z = 5.78 mm.

The precession has been found to be counter-clockwise for positive *m* and clockwise for negative *m*, requiring a distance of 3.2 mm for one revolution of the profile for the $m = 1$ case. This strongly suggests that the origin of this behavior stems from the observation that the Pointing vector for eigenmodes of nonzero angular momentum is not entirely along the propagation direction, but has an additional component along the θ direction, due to the $e^{im\theta}$ dependence of the fields. Thus, power flow (even when the mode is cylindrically symmetric) follows a spiral path with an angle from the z axis given by $\tan\varphi = m / rk$. This leads immediately to the simple formula for the propagation length required for one complete revolution as

$$z_{1rev} = \frac{4\pi^2 r^2 \overline{n}}{m\lambda_0} \tag{8}$$

For the $m = 1$ case shown above, predictions from Eq. (8) range from 2.1 mm to 8.4 mm for values of *r* ranging from half the core radius to one core radius, resp. These values bracket the numerical results and thus reinforce the conclusion that the inherent angular momentum of the beam is responsible for the precession behavior.

It should be mentioned that in the course of the simulation, the profiles do not remain as symmetric and regular as those shown in Fig. 3, but rather become less ordered and unpredictable. In particular, most of the energy often winds up in a single lobe, which for powers above P_{cr} usually results in self-focusing.

An immediate and obvious question arises as to whether the precession phenomenon just described might inhibit self-focusing. One plausible mechanism for this assertion involves the spiral motion of the major lobes. Self-focusing results when the index “lens” formed around an intensity peak focuses the light, further intensifying the lens, provided the beam is propagating in a straight line. For light propagating in a spiral path, the lobe might move away from the lens if the spiral is tight enough compared with the distance to the self-focus. Since self-focusing generally happens in the space of a few hundred microns, the spiral above that requires over 3 mm to complete is not expected to have a large effect on self-focusing behavior. However, modes with larger *m*, say between 5 and 10, might be expected to show a more sizeable effect.

Finally, an attempt was made to quantify the influence of angular momentum on the resistance of the beam to self-focusing. Normally, one would proceed by doing a series of calculations at increasingly higher power until a self-focusing event occurred. Performing a set of such calculations for each value of angular momentum (or topological charge) would then yield a useful plot of maximum propagating power *vs*. *m*. In this case, this procedure was not practical due to a lack of conservation of both beam energy and (especially) angular momentum during propagation over such long distances (typically 10^4 propagation steps). Instead, we found it more useful to propagate the different modes starting with the same initial power and recording the distance to a self-focusing event. The results of this exercise are shown in Fig. 4.

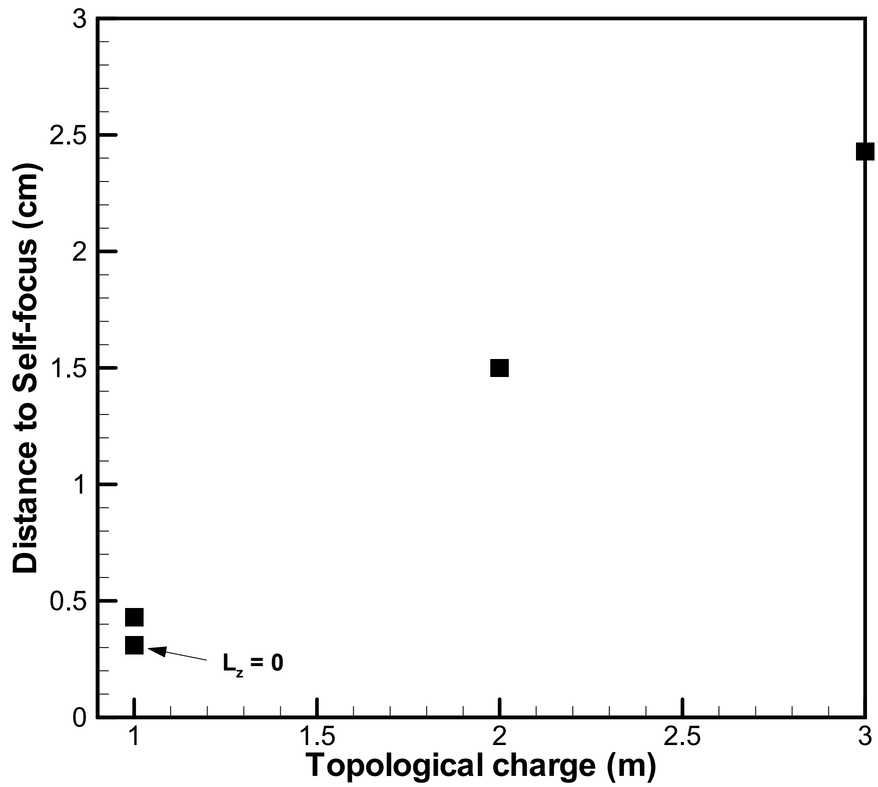

Fig. 4 Distance to self-focus *vs* topological charge (*m*). The initial beam power was constant at 9 MW. Each beam was initially cylindrically symmetric in amplitude (except for the point marked $L_z = 0$).

For these calculations a larger problem region of 52 μm was used along with a finer mesh of 0.15 μm inside the core by increasing the number of grid points to 260 x 260 and employing the variable zoning capabilities of the triangular mesh generator. In each case the beam power was adiabatically ramped up to 9 MW and the modal behavior observed. For the two $m = 1$ cases, self focusing occurred quickly before any loss of energy or angular momentum took place. For the beam with zero angular momentum, the two pre-existing lobes self-focused immediately after the total power exceed $2P_{cr}$ as expected. The non-zero angular momentum case behaved similarly, except that the cylindrically-symmetric profile first evolved into two precessing lobes as described above, but these then self-focused within one mm.

For the higher values of *m*, two precessing lobes were produced in both cases (but with faster precession rates than listed above for $m = 1$). Self-focusing was inhibited so long as these lobes remained distinct and positioned on opposite sides of the fiber. However, eventually in both cases the lobes moved closer together and exchanged energy, with self-focusing following as soon as the energy was concentrated primarily in one of the lobes. For the $m = 2$ case, the energy had decreased to 8.38 MW and the topological charge to 1.3 by the time self-focusing occurred. For the $m = 3$ case, the energy dropped to 7.7 MW and the charge to 1.4 due to the longer propagation length.

The conclusions presented here concerning the effects of angular momentum on self-focusing must be acknowledged as preliminary, due to our inability to propagate beams with nonzero topological charge for long distances without a (presumably numerical) loss of angular momentum. A future follow-on investigation will require more sophisticated beam propagation models that conserve both energy and angular momentum accurately even in the presence of the Kerr nonlinearity. However, it appears that higher angular momentum states do mitigate self-focusing to some degree by inhibiting the coalescence of multiple lobes into a single lobe, thus distributing the power between the lobes. Of course, we have not checked this hypothesis for values of m above 3 due to the required mesh refinements and the concomitant increase in numerical effort. It is possible that the spiral paths followed by each precessing lobe inhibit self-focusing also, as illustrated by the longer distance to focus for the $m = 1$ mode with angular momentum shown in Fig. 4, compared with the zero angular momentum mode.

IV. Conclusion

We have performed an investigation into the influence of angular momentum on self-focusing behavior for the first few lowest-order fiber modes. This was done using a triangular mesh beam propagation code capable of accurately resolving both the cylindrical fiber core shape and the beam amplitude and phase. The index of refraction was continually updated during propagation in order to investigate the behavior of the propagating mode in a Kerr medium. Conclusions drawn from this investigation may be summarized as (1) a single-lobed mode propagating in the fiber will self-focus at a power equal to the critical power for bulk media P_{cr}; (2) higher-order fiber modes without angular momentum cannot substantially increase this power despite being multi-lobed because the presence of the nonlinearity leads to coalescence into a single lobe; (3) Higher-order "vortex" modes with angular momentum inhibit self-focusing by mechanisms that are not entirely understood, but we suspect mostly by preventing the multiple precessing lobes from coalescing, thus scaling the allowable power by the number of lobes.

V. Acknowledgement

This work was performed at Sandia National Laboratories. Sandia is a multiprogram laboratory operated by Sandia Corporation, a Lockheed Martin Company, for the United States Department of Energy's National Nuclear Security Administration under contract DE-AC04-94AL85000.

VI. References

1. J. A. Fleck, Jr., and C. Layne, “Study of self-focusing damage in a high power Nd:glass-rod amplifier”, Appl. Phys. Lett., 22, 467-469(1973).
2. J. H. Marburger, “Self-focusing: Theory”, Prog. In Quantum Electr. 4, 35-110, Pergamon Press (1975).
3. L. T. Vuong, T. D. Grow, A. Ishaaya, A. L. Gaeta, G. W. ‘t Hooft, E. R. Eliel and G. Fibich, “Collapse of Optical Vortices”, Phys. Rev. Lett. 96, 133901(2006).
4. G. R. Hadley, R. L. Farrow, and A. V. Smith, “Three-dimensional, time-dependent modeling of high-power fiber amplifiers”, paper 6453-47, LASE 2007.
5. G. R. Hadley, “Wide-angle beam propagation using Pade approximant operators”, Opt. Lett. 17, 1426-1428(1992).
6. G. R. Hadley, “Numerical Simulation of Waveguides of Arbitrary Cross-Section”, Int. J. Electron. Commun. (AEU)58, 86-92(2004).
7. Classical Electrodynamics, J. D. Jackson, John Wiley & Sons, New York, 1962, p.542.